THERMO-HYDRAULIC MODELLING OF DIRECT STEAM GENERATION IN A SOLAR PARABOLIC TROUGH COLLECTOR SYSTEM

Bohra Nitin Kumar and K S Reddy*
Heat Transfer and Thermal Power Laboratory,
Department of Mechanical Engineering,
Indian Institute of Technology Madras, Chennai-600 036, India
*Corresponding author Tel. +91-44-2257 4702
E-mail: ksreddy@iitm.ac.in

ABSTRACT

Direct steam generation using a solar parabolic trough collector for industrial process heat is gaining ground owing to the improved system performance and economic benefits. The major challenges in the design of a feasible parabolic trough collector system for the direct steam generation process are the large pressure losses in the evaporating section and the high thermal gradients in the absorber tube. The numerical results of a sensitivity study based on a thermo-hydraulic model for saturated steam generation in a small-sized solar parabolic trough collector are analyzed. In the present study, a solar parabolic trough collector system with aperture width of 0.84 m, focal length of 0.3 m and absorber tube with an inner diameter of 0.02 m is considered. For accuracy, the complex two-phase flow in the evaporating section of the collector field is analyzed using a flow pattern map integrated heat transfer and pressure drop models. The effect of inlet water temperature, pressure, mass flow rate and direct solar irradiance on pressure loss, flow pattern distribution, outlet temperature, and dryness fraction is investigated. For inlet pressure of 1 MPa, a significant pressure drop of 444.48 kPa (about 44.5% of inlet pressure) is found at direct solar irradiance of 900 W/m^2 and mass flow rate of 0.06 kg/s. The transition from stratified-wavy to annular flow pattern on the left-hand side of the flow pattern map occurs at dryness fraction of 0.28, 0.33 and 0.39 for inlet pressure of 1.0, 1.5 and 2 MPa respectively. Lower inlet pressures are found favorable for an early transition to annular flow pattern. However, significant pressure drop at lower operating pressure may play a crucial role in the viability of using small-sized parabolic trough collector systems for saturated steam generation.

INTRODUCTION

Direct steam generation (DSG) in a solar parabolic trough collector for industrial process heat improves the performance and reduces the cost involved. In the DSG process water is used as the working fluid in the solar field in place of synthetic oil. The advantages of direct steam generation process are simple integration, reduced working fluid cost, improved solar field efficiency, and reduced capital cost. The water flowing through the absorber tube is initially preheated to the saturation temperature and then the evaporation occurs. The thermo-hydraulic modelling of the two-phase flow is complex due to the interaction between the phases, flow transitions and instabilities, and interface motion. Moreover, an accurate thermo-hydraulic model of the two-phase flow in the absorber tube helps in the detailed design of the DSG based solar collector field [1]. A closed form analytical model predicting the temperature profiles of heat transfer fluid, absorber wall and glass envelope was developed for modelling the DSG process by Xu and Wiesner [2]. However, the results obtained from the analytical model were found to be approximate. Odeh et al. [3] developed a steady state hydrodynamic model for the DSG process using an extrapolated adiabatic flow pattern map and an empirical pressure drop correlation. Eck and Steinmann [4] considered only the stratified to annular flow transition in the model developed for the DSG process in a solar PTC. Reddy and Kumar [5] carried a feasibility study based on geometrical parameters, collector configuration and solar radiation for a stand-alone PTC using water and oil as working fluid. The degree of sensitivity to DSG factors for PTC's with small diameter receiver tubes is high owing to the strong thermo-hydraulic coupling [6]. The pressure losses for generating pressurized hot water in a solar PTC are small in comparison to the working pressure. Whereas, the pressure losses may be quite significant when PTC's with small diameter receiver tubes are used for generation of saturated steam. The pressure drop in the absorber tube is a critical criterion for the feasibility of saturated steam generation in small-sized solar PTC systems. Moreover, the strong thermo-hydraulic coupling and the necessity to identify the critical process conditions in the evaporating section of the absorber tube, an accurate thermo-hydraulic model is required.

In the present work, a thermo-hydraulic model is developed using flow pattern map integrated heat transfer and pressure drop correlations for predicting the thermo-hydraulic aspects of the two-phase flow in the evaporating section. Apart from the thermo-hydraulic aspects, the model also evaluates the temperature of the absorber wall, glass cover and heat loss from the absorber along the length of the collector. Further, a sensitivity study for saturated steam generation in a small-sized PTC system is carried out. Inlet pressure, temperature, mass flow rate, and direct normal irradiance were the parameters used for the sensitivity study. The results of varying the inlet parameters on pressure drop, dryness fraction, outlet temperature and flow pattern transitions are discussed.

NOMENCLATURE

A_{ap}	[m^2]	Aperture area
f	[-]	Friction factor
G	[kg/m^2s]	Mass velocity
h	[W/m^2K]	Heat transfer coefficient
k	[W/mK]	Thermal conductivity
p	[M Pa]	Pressure
q''	[W/m^2]	Local heat flux
T	[^oC]	Temperature

Special characters

ϵ	[-]	Emissivity
ϵ	[-]	Vapour void fraction
δ	[m]	Liquid film thickness
θ	[degrees]	Refers to angle
μ	[Pa s]	Dynamic viscosity
ρ	[kg/m^3]	Density
σ	[W/m^2K^4]	Stefan-Boltzmann constant

Subscripts

a	Absorber tube
c	Glass cover
i	Inner
L	Refers to liquid phase
o	Outer
V	Refers to vapour phase

THERMO-HYDRAULIC MODEL

In the present study, a steady state one-dimensional thermo-hydraulic model based on energy balance between the heat transfer fluid, receiver tube, and the surroundings is developed. The primary components of the solar parabolic trough collector and the energy balance across the receiver tube is illustrated in Figure1 and Figure 2 respectively. The amount of energy absorbed by the receiver of PTC is given by the equation (1)

$$\dot{Q}_{abs} = A_{ap}\, DNI\, cos\phi\ \ \eta_{opt}\, IAM\, F \tag{1}$$

Where A_P is the aperture area of the collector, *DNI* is direct normal irradiance, ϕ is the angle of incidence, η_{opt} is the optical efficiency, *IAM* is the incidence angle modifier and *F* is the soiling factor. The angle of incidence (ϕ), is the angle a ray of sun makes with a normal to the reflector surface. However, the amount of energy gained by the fluid inside the absorber tube is less due to optical and thermal losses. The amount of energy gained by the fluid is the difference between the energy absorbed and the energy loss and is given by equation (2).

$$\dot{Q}_{gain} = \dot{Q}_{abs} - \dot{Q}_{loss} \tag{2}$$

The energy loss from the receiver may be attributed to the radiative loss in the annular space between the absorber surface and glass cover or the convective and radiative loss from the glass envelope to the surroundings. The energy loss from the receiver can be given by any of the equations (3) or (4) [3].

$$\dot{Q}_{loss} = \pi D_{a,o} L\sigma \frac{T_{a,o}^4 - T_{c,i}^4}{1/\varepsilon_a + D_{a,o}/D_{c,i}\left(\frac{1-\varepsilon_a}{\varepsilon_a}\right)} \tag{3}$$

$$\dot{Q}_{loss} = \pi D_{c,o} L h_w \left(T_{c,o} - T_{amb}\right) + \pi D_{c,o}\sigma\varepsilon_c\left(T_{c,o}^4 - T_{sky}^4\right) \tag{4}$$

Here, T_{amb}, T_{sky}, $T_{a,o}$, $T_{c,i}$, and $T_{c,o}$ represent the ambient, sky, absorber outer surface, and glass cover inner and outer surface temperatures respectively. The numerical model is based on discretizing the length of the absorber tube into sections, and are further divided into sub-sections. The inlet conditions of temperature and pressure are used to find the outlet conditions iteratively and are fed as input for the subsequent subsection. In the preheating section, single phase heat transfer and pressure drop correlations are used and in the evaporating section flow pattern map integrated two-phase correlations are utilized. A FORTRAN code is developed for the thermo-hydraulic modelling of saturated steam generation in the solar PTC. The thermo-hydraulic model estimates the temperature profiles of absorber wall, glass cover, mean fluid temperature, pressure drop, dryness fraction, and heat transfer coefficients along the collector length.

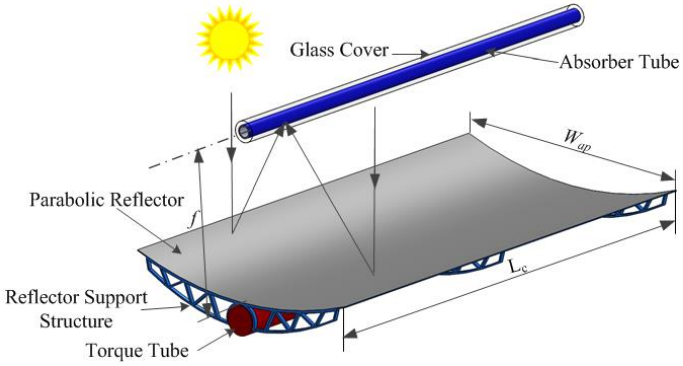

Figure 1 Primary components of a solar PTC

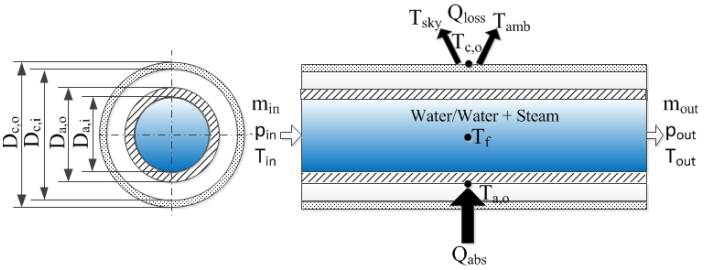

Figure 2 Energy balance across the receiver tube

Single Phase Flow

In the direct steam generation process, water is preheated, evaporated and superheated along the length of the collector. In the present study, the preheating of water and generation of saturated steam in a solar parabolic trough collector is carried out. The heat transfer coefficient in the preheating section of the collector field is found using the Gnilienski correlation, given as:

$$Nu_D = \frac{\left(f/8\right)\left(Re_D - 1000\right)Pr_L}{1 + 12\left(f/8\right)^{0.5}\left(Pr_L^{2/3} - 1\right)}\left(\frac{Pr_L}{Pr_w}\right)^{0.11} \tag{5}$$

where, $f = (1.82log_{10}Re_D - 1.64)^{-2}$ (6)

The single phase pressure drop along the length of the preheating section is determined using the Darcy-Wiesbach equation given by equation (7). The friction factor, f_L for the absorber tube with surface roughness ε for a turbulent flow is given by the equation (8).

$$\Delta p_L = \frac{f_L L}{D}\left(\frac{\rho_L u_L^2}{2}\right) \tag{7}$$

$$\text{where, } f_L = 0.0055 \times \left[1 + \left(20{,}000 \times \frac{\varepsilon}{D} + \frac{10^6}{Re_D}\right)^{1/3}\right] \tag{8}$$

Two Phase Flow

The optimization of thermal systems involved with two-phase flow is based on reliable prediction of the thermo-hydraulic behaviour. In the present study, Wojtan et al. [7, 8] flow pattern map integrated heat transfer and pressure drop models are used to analyse the thermo-hydraulic behaviour of the two-phase flow during the saturated steam generation. The heat transfer model considers the heat transfer in the lower wet perimeter and the upper dry perimeter for calculating the heat transfer coefficient (see Figure 3), given as:

$$h_{tp} = \frac{\theta_{dry} h_{dry} + (2\pi - \theta_{dry}) h_{wet}}{2\pi} \tag{9}$$

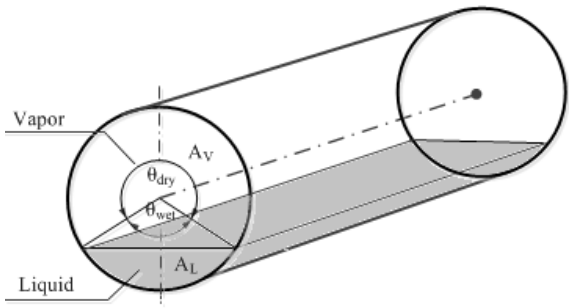

Figure 3 Tube with stratified two-phase flow [7].

In equation (9), h_{dry} and h_{wet} are the heat transfer coefficients relating to the dry and wet perimeters inside the tube respectively. The heat transfer coefficients in the dry and wet perimeter are given by the equations (10) and (11) respectively.

$$h_{dry} = 0.023 \times Re_V^{0.8} Pr_V^{0.4} \frac{k_V}{D_i} \tag{10}$$

$$h_{wet} = (h_{cb}^3 + h_{nb}^3)^{1/3} \tag{11}$$

The contributions from the nucleate and convective boiling in the wet perimeter are given by equations (12) and (13)

$$h_{cb} = 0.0133 \times Re_\delta^{0.69} Pr_L^{0.4} \frac{k_L}{\delta} \tag{12}$$

$$h_{nb} = 55 \times P_R^{0.12} (-\log_{10}(P_R))^{-0.55} M^{-0.5} q^{0.67} \tag{13}$$

where $Re_\delta = \frac{4G\delta(1-x)}{\mu_L(1-\epsilon)}$, $P_R = p/p_{crit}$ (p_{crit} is critical pressure), δ is the film thickness and M is the molecular weight. However, the heat transfer coefficients in the dry and mist region are treated differently (refer [7, 8]). The values of θ_{dry}, which depend on the flow pattern are found using Table 1.

Table 1: Flow pattern based values of dry angle [7].

Flow pattern	Dry angle
Stratified	$\theta_{dry} = \theta_{strat}$
Slug, Intermittent and Annular	$\theta_{dry} = 0$
Slug + Stratified-wavy	$\theta_{dry} = \left(\frac{x}{x_{IA}}\right)\left(\frac{G_{wavy} - G}{G_{wavy} - G_{strat}}\right)^{0.61} \theta_{strat}$
Stratified-wavy	$\theta_{dry} = \left(\frac{G_{wavy} - G}{G_{wavy} - G_{strat}}\right)^{0.61} \theta_{strat}$

The total two-phase pressure drop in a horizontal tube is expressed as:

$$\Delta p_{total} = \Delta p_{mom} + \Delta p_{frict} \tag{14}$$

Where, Δp_{mom} is the momentum pressure drop due to the flow acceleration in a diabatic flow [9] and is calculated using equation (15).

$$\Delta p_{mom} = G^2 \left[\left\{\frac{(1-x)^2}{\rho_L(1-\epsilon)} + \frac{x^2}{\rho_V \epsilon}\right\}_{out} - \left\{\frac{(1-x)^2}{\rho_L(1-\epsilon)} + \frac{x^2}{\rho_V \epsilon}\right\}_{in}\right] \tag{15}$$

Where x is the dryness fraction, ϵ is cross sectional vapour void fraction, and G is the total mass velocity. The frictional pressure drop Δp_{frict}, predicted using the empirical or semi-empirical correlations is of limited reliability due to the complexity of the two-phase flow. The predicted pressure drop may differ by 50% or more and due to the strong coupling of the thermo-hydraulic behaviour, the accurate prediction of pressure drop is critical for the optimization of the system. In the present study the flow pattern map integrated pressure drop models by Quiben et al. [9, 10] are utilized to find the frictional pressure drop in the evaporating section of the collector field. The pressure drop models consider the flow patterns existing in the absorber tube to evaluate the pressure drop accordingly.

System Description and Parameters for Sensitivity Study

For the present study, a small-sized solar parabolic trough collector system is considered for saturated steam generation.

The collector field is sized for preheating of water and generation of saturated steam for industrial process heat. The details of the solar collector system are illustrated in Table 2. The developed thermo-hydraulic model is used to carry out a sensitivity study for the saturated steam generation in the small-sized solar PTC. The collector field is designed for industrial process steam in the temperature range of 150 ºC -225 ºC .The effect of varying the inlet mass flow rate, pressure, temperature and direct normal irradiance on the dryness fraction, outlet temperature, pressure drop, flow pattern transitions in the absorber tube and flow pattern map is analyzed. The values of the inlet parameters considered for the sensitivity study are illustrated in Table 2.

Table 2: Characteristics of the PTC and inlet parameters

Parameter	Value
Aperture width (W)	0.840 m
Focal length (f)	0.300 m
Collector length (L_c)	1.000 m
Absorber inner diameter ($D_{a,i}$)	0.020 m
Absorber outer diameter ($D_{a,o}$)	0.022 m
Glass cover inner diameter ($D_{c,i}$)	0.032 m
Glass cover outer diameter ($D_{c,o}$)	0.034 m
Emissivity of absorber (ε_a)	0.10
Emissivity of glass cover (ε_c)	0.88
Glass tube transmittance (τ)	0.96
Absorber tube absorptance (α_a)	0.92
Specular reflectance of mirror(ρ)	0.91
Total number of collectors	216
Number of loops	3
Modules per loop	3
Collectors per module	24
Inlet mass flow rate ($\dot{m}_{in}$)	[0.050, 0.055, 0.060] kg/s
Direct normal irradiance (DNI)	[450, 600, 750, 900] W/m^2
Inlet pressure (p_{in})	[1.0, 1.5, 2.0] MPa
Inlet temperature (T_{in})	[80, 90, 100] ºC

RESULTS AND DISCUSSION

The results of varying the inlet parameters on the pressure drop, dryness fraction, outlet temperature and flow pattern transitions in the absorber tube are presented in this section.

Effect of Inlet Pressure and DNI on Outlet Parameters

The effect of varying the inlet pressure and DNI for an inlet mass flow rate of 0.060 kg/s and inlet temperature of 100 ºC on pressure drop, dryness fraction, and outlet temperature is illustrated in Figure 4. As shown in the Figure 4(a), for a given DNI the pressure drop is found to be quite large for low operating pressures. For inlet pressure of 1 MPa, a significant pressure drop of 444.80 kPa (about 44.5 % of inlet pressure) is found at a DNI of 900 W/m^2. Whereas, for the same DNI and inlet pressure of 2 MPa a pressure drop of 172.68 kPa (less than 10% of inlet pressure) is found. Therefore, it may be concluded that inlet pressure plays a crucial role for the feasibility of solar PTC systems for saturated steam generation. As shown in Figure 4(b) for a given inlet pressure, the dryness fraction increases with DNI but, with an increase in inlet pressure at a given DNI the dryness fraction decreases owing to the increase in the preheating required to reach the saturation temperature. At inlet pressure of 1, 1.5 and 2 MPa, dryness fraction illustrates a decreasing trend with values of 0.32, 0.29 and 0.26 respectively for DNI of 450 W/m^2. In Figure 4(c), the outlet temperature, for DNI of 750 W/m^2 is found to increase from 165.42 ºC to 209.40 ºC with an increase in inlet pressure from 1 MPa to 2 MPa respectively. The increase in outlet temperature may be attributed to saturation temperature at given pressure and pressure drop along the length of the absorber tube.

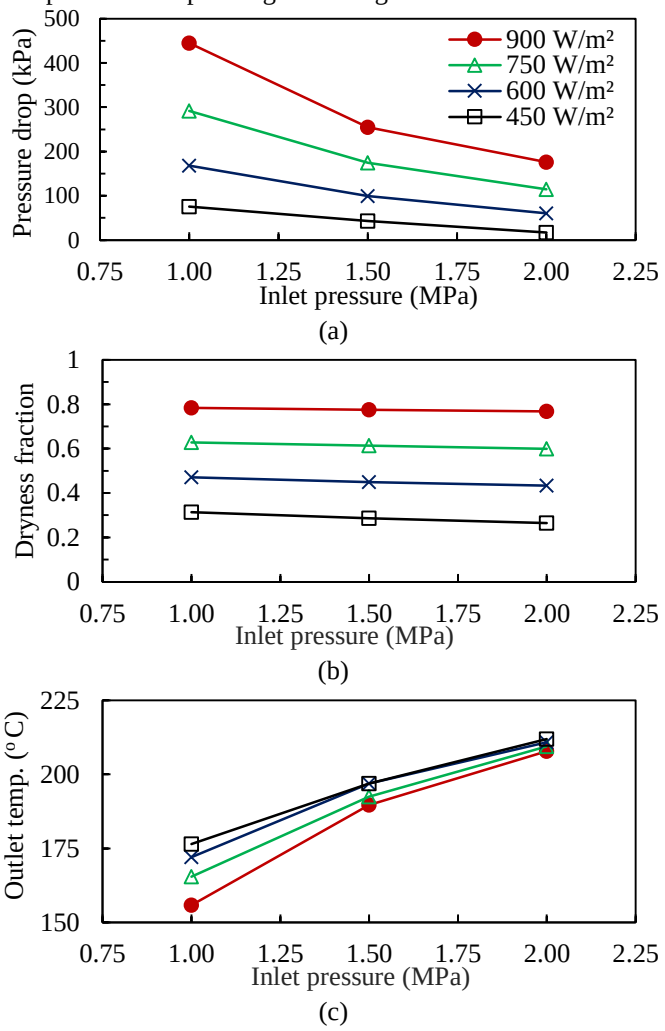

Figure 4 Effect of inlet pressure and DNI on (a) pressure drop (b) dryness fraction and (c) outlet temperature

Effect of Inlet Mass Flow Rate and Temperature on Outlet Parameters

The effect of varying the inlet mass flow rate and temperature on the outlet parameters is illustrated in Figure 5. The variation in pressure drop, dryness fraction, and outlet temperature are plotted for an inlet pressure of 1 MPa and DNI of 900 W/m^2. In the preheating section, the pressure drop is proportional to the square of velocity and in the two-phase region, a higher order proportionality exists between the pressure drop and velocity. As illustrated in Figure 5(a), at an inlet temperature of 90 ºC there is an increase in the pressure drop from a value of 326.50 kPa to 418.43 kPa with an increase in mass flow rate from 0.05 kg/s to 0.06 kg/s. Moreover, the

pressure drop also increases with increase in inlet temperature at a given mass flow rate. The increase in pressure drop may be attributed to reduction in preheating requirement and increase in the length of the evaporating section. Figure 5(b) illustrates, an increase in the dryness fraction with an increase in the inlet temperature for a given mass flow rate. The increase in dryness fraction may be due to reduction in preheating temperature. In Figure 5(c) a fall in the outlet temperature is found with increasing mass flow rate for a given inlet temperature.

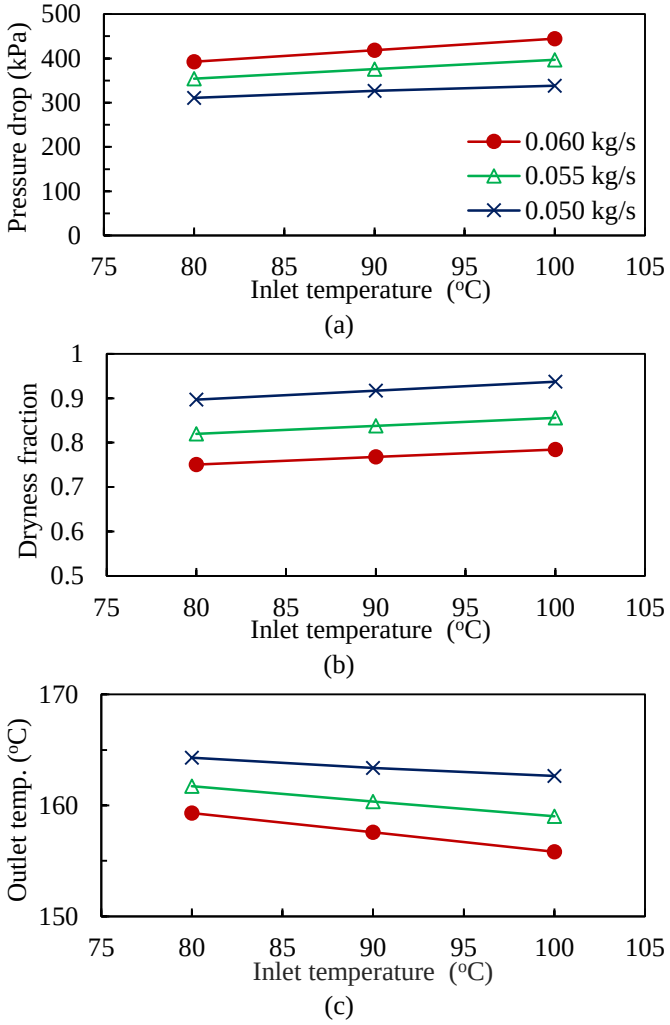

Figure 5 Effect of inlet temperature and mass flow rate on (a) pressure drop (b) dryness fraction and (c) outlet temperature

Influence of Inlet Pressure on Flow Pattern Map and Flow Pattern Distribution

The result of varying the inlet pressure on the flow pattern map is shown in Figure 6(a). The transition from slug to annular flow for high mass flux occurs at high dryness fraction with an increase in inlet pressure. For inlet pressure of 1.0, 1.5 and 2.0 MPa, the transition boundary is found at dryness fraction of 0.17, 0.22 and 0.26 respectively for an inlet temperature of 100 °C and mass flow rate of 0.05 kg/s. Similarly, the transition from slug to slug + stratified-wavy and from stratified-wavy to annular flow pattern on the left-hand side of the flow pattern map occurs at higher dryness fraction with an increase in the inlet pressure. The transition from stratified-wavy to annular flow pattern on the left-hand side of the flow map occurs at dryness fractions of 0.28, 0.33 and 0.39 for inlet pressure of 1.0, 1.5 and 2 MPa respectively. Moreover, at higher and lower mass velocities the substantial shifts in the slug to intermittent flow and slug + stratified-wavy to stratified-wavy flow patterns will be effective.

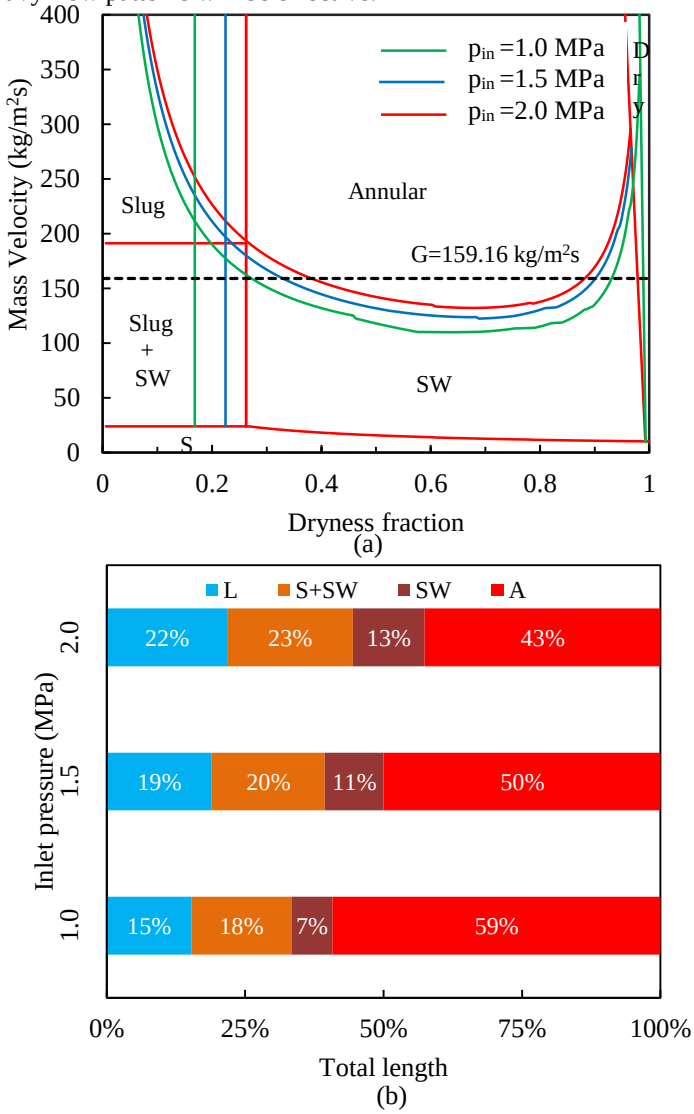

Figure 6 Influence of inlet pressure on (a) flow pattern map and (b) flow pattern distribution

The result of inlet pressure on the flow pattern distribution inside the absorber tube is illustrated in Figure 6(b). The length occupied by annular flow inside the absorber tube increases from 43% to 59%, for decrease in the inlet pressure from 2.0 MPa to 1.0 MPa. The increase in the length occupied by annular flow pattern may be attributed to the reduction in preheating, and the transition to annular flow occurring at lower dryness fraction for inlet pressure of 1MPa. It is clear from the flow pattern map, that low inlet pressures are favourable for increasing the occupation length of annular flow inside the absorber tube. However, a large pressure drop of 444.80 kPa for inlet pressure of 1 MPa offsets the incentive of increase in the length occupied by annular flow pattern.

Influence of Inlet Temperature on Flow Pattern Map and Flow Pattern Distribution

For an inlet pressure of 1MPa, DNI of 900 W/m^2 and mass flow rate of 0.05 kg/s the effect of varying the inlet temperature on flow pattern map is shown in Figure 7(a). There is no variation in the transition boundaries of the flow pattern map at different inlet temperatures. The flow pattern distribution inside the absorber tube for different inlet temperatures is illustrated in Figure 7(b). An increase from 56 % to 59 % is observed for the length occupied by annular flow pattern for an inlet temperature of 80 ºC and 100 ºC respectively. The increase in the annular flow pattern occupation length is due to the decrease in the preheating required to reach the saturation temperature.

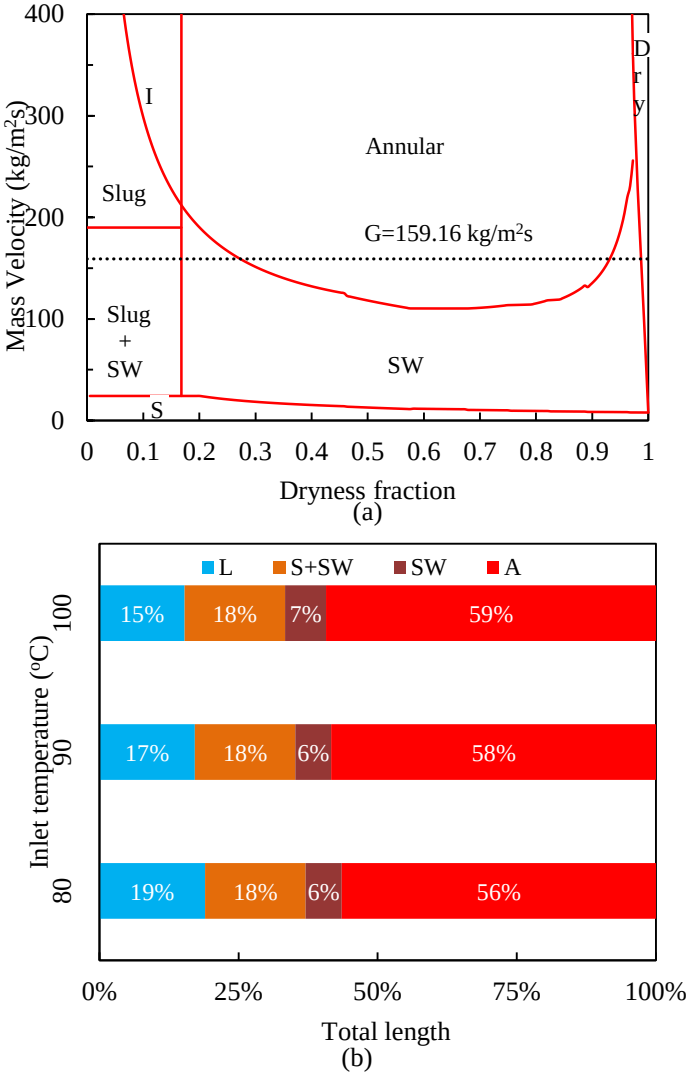

Figure 7 Influence of inlet temperature on (a) flow pattern map and (b) flow pattern distribution

CONCLUSIONS

In the present study, flow pattern map integrated heat transfer and pressure drop models are used to develop a thermo-hydraulic model for the saturated steam generation process in a solar PTC. Further, a sensitivity study is carried for saturated steam generation by analysing the effects of varying the inlet temperature, pressure, mass flow rate and direct solar irradiance on the outlet parameters. A small sized PTC with an aperture width of 0.84 m, focal length of 0.3 m and inner absorber diameter of 0.02 m is selected for the sensitivity study. The collector field is designed for generation of saturated steam for industrial process heat in the range of 150 ºC to 225 ºC. The results of varying the inlet parameters on the pressure drop, outlet temperature, and dryness fraction are reported. Moreover, the effect of varying inlet pressure and temperature on the flow pattern map and the flow pattern distribution inside the absorber tube is also presented. At inlet pressure of 1MPa, a significant pressure drop of 444.8 kPa is found for mass flow rate of 0.06 kg/s and DNI of 900 W/m2. The transition from stratified-wavy to annular flow pattern on the left-hand side of the flow pattern map occurs at dryness fraction of 0.28, 0.33 and 0.39 for inlet pressure of 1.0, 1.5 and 2 MPa respectively. Low inlet pressure is found favourable for an early transition from slug + stratified-wavy to annular flow. However, the pressure drop at low inlet pressure is found to be very significant and may play a crucial role in the feasibility of using small sized solar PTC for saturated steam generation.

REFERENCES

[1] D. Lobon, E. Baglietto, L. Valenzuela, and E. Zarza, "Modeling direct steam generation in solar collectors with multiphase CFD," *Applied Energy*, vol. 113, pp. 1338–1348, 2014.

[2] R. Xu and T. Wiesner, "Closed-form modeling of direct steam generation in a parabolic trough solar receiver," *Energy*, vol. 79, pp. 163–176, 2015.

[3] S. D. Odeh, G. L. Morrison, and M. Behina, "Modeling of parabolic trough direct steam generation solar collectors," *Solar Energy*, vol. 62, no. 6, pp. 395–406, 1998.

[4] M. Eck and W. D. Steinmann, "Modelling and design of direct solar steam generating collector fields," *Journal of Solar Energy Engineering, Transactions of the ASME*, vol. 127, no. 3, pp. 371–380, 2005.

[5] K S Reddy and K Ravi Kumar, "Solar collector field design and viability analysis of stand-alone parabolic trough power plants for Indian conditions," *Energy for Sustainable Development*, vol. 16, pp. 456-470, 2012.

[6] R. Silva, M. Perez, M. Berenguel, L. Valenzuela, and E. Zarza, "Uncertainty and global sensitivity analysis in the design of parabolic-trough direct steam generation plants for process heat applications," *Applied Energy*, vol. 121, pp. 233–244, 2014.

[7] L. Wojtan, T. Ursenbacher, and J. R. Thome, Investigation of flow boiling in horizontal tubes: Part I - A new diabatic two-phase flow pattern map," *International Journal of Heat and Mass Transfer*, vol. 48, no. 14, pp. 2955–2969, 2005.

[8] L. Wojtan, T. Ursenbacher, and J. R. Thome, Investigation of flow boiling in horizontal tubes: Part II - Development of a new heat transfer model for stratified-wavy, dryout and mist flow regimes," *International Journal of Heat and Mass Transfer*, vol. 48, no. 14, pp. 2970–2985, 2005.

[9] J. Moreno Quiben and J. R. Thome, "Flow pattern based two-phase frictional pressure drop model for horizontal tubes, Part I: Diabatic and adiabatic experimental study," *International Journal of Heat and Fluid Flow*, vol. 28, no. 5, pp. 1049–1059, 2007.

[10] J. Moreno Quiben and J. R. Thome, "Flow pattern based two-phase frictional pressure drop model for horizontal tubes, Part II: New phenomenological model," *International Journal of Heat and Fluid Flow*, vol. 28, no. 5, pp. 1060–1072, 2007.